Acta Oceanol. Sin., 2019, Vol. 38, No. 1, P. 48–60
https://doi.org/10.1007/s13131-019-1369-7
http://www.hyxb.org.cn
E-mail: hyxbe@263.net

Dynamic of ENSO towards upwelling and thermal front zone in the east coast of Peninsular Malaysia

Nurul Rabitah Daud[1, 2], Mohd Fadzil Akhir[1]*, Aidy M Muslim[1]

[1] Institute of Oceanography and Environment, Universiti Malaysia Terengganu, Terengganu 21030, Malaysia

[2] Faculty of Civil Engineering, Universiti Teknologi MARA, Selangor 40450, Malaysia

Received 30 August 2017; accepted 13 January 2018

Abstract

The El Niño Southern Oscillation (ENSO) is a natural phenomenon that relates to the fluctuation of temperatures over the Pacific Ocean. The ENSO significantly affects the ocean dynamics including upwelling event and coastal front. A recent study discovered the seasonal upwelling in the east coast of Peninsular Malaysia (ECPM), which is significant to the fishery industry in this region. Thus, it is vital to have a better understanding of the influence of ENSO towards the coastal upwelling and thermal front in the ECPM. The sea surface temperature (SST) data achieved from moderate resolution imaging spectroradiometer (MODIS) aboard Aqua satellite are used in this study to observe the SST changes from 2005 to 2015. However, due to cloud cover issue, a reconstruction of data set is applied to MODIS data using the data interpolating empirical orthogonal function (DINEOF) to fill in the missing gap in the dataset based on spatial and temporal available data. Besides, a wavelet transformation analysis is done to determine the temperature fluctuation throughout the time series. The DINEOF results show the coastal upwelling in the ECPM develops in July and reaches its peak in August with a clear cold water patch off the coast. There is also a significant change of SST distribution during the El Niño years which weaken the coastal upwelling event along the ECPM. The wavelet transformation analysis shows the highest temperature fluctuation is in 2009–2010 which indicates the strongest El Niño throughout the time period. It is suggested that the El Niño is favourable for the stratification in water column thus it is weakening the upwelling and thermal frontal zone formation in ECPM waters.

Key words: ENSO, thermal frontal zone, coastal upwelling, sea surface temperature, South China Sea

Citation: Daud Nurul Rabitah, Akhir Mohd Fadzil, M muslim Aidy. 2019. Dynamic of ENSO towards upwelling and thermal front zone in the east coast of Peninsular Malaysia. Acta Oceanologica Sinica, 38(1): 48–60, doi: 10.1007/s13131-019-1369-7

1 Introduction

The sea surface temperature (SST) provides a comprehensive understanding in biological and physical oceanography of marine ecosystem. This has increased focus and effort to examine the changes of SST that is particularly related with coastal front and upwelling event. The SST is an indicator to interpret the dynamic of coastal front and upwelling events which are related to the area of high biological activities in the marine ecosystem. SST is also influenced by monsoon seasons, thus it becomes a good indicator in the marine environment.

The southern South China Sea (SCS) is largely dominated by the northeast monsoon from November to February with strong northeasterly wind blows over this region. During the northeast monsoon season, this region receives heavy rain, cloud cover and strong southward current along the coast resulting in bad weather conditions impacting fishery industry. The southwest monsoon from June to September drives northward current along the east coast of Peninsular Malaysia (ECPM) coast. This monsoon season cools down the ECPM region after the dry period normally strikes between April and May. The fishery industry also improves during this season by the presence of coastal upwelling at the ECPM due to northward current.

The previous study done by Phuoc et al. (2002) reported the presence of upwelling event in the ECPM and a detailed research has been conducted by Akhir et al. (2015) in order to provide better information and evidence on this coastal upwelling. However, there is still a gap in understanding the dynamic and scale of this coastal upwelling. Thus, this study attempts to provide information on the coastal upwelling event using satellite imagery SST dataset.

Satellite remote sensing provides information on SST at moderate resolution (~4 km), cover a large area and longer time series. Many researchers have proved the effectiveness of satellite remote sensing data in order to provide information for the seas and oceans studies (Kok et al., 2015; Moradi and Kabiri, 2015; Khalil et al., 2016; He et al., 2016). Most of these studies focused on hydrodynamics, upwelling, coastal front, distribution and variability of SST, which cover large area of seas and a long period of time.

The application of satellite remote sensing data usually encounters excessive cloud cover issue, specifically in the area located close to the equator. This issue is getting worse during the monsoon seasons. For each season, it takes a few months to end and most regions experience two monsoon seasons throughout a year. This reflects the less availability of daily, weekly and monthly satellite data for equatorial region compared to the higher latitude regions. Regarding solving the issue, the focus has been dragged to synchronous variations of SST by applying several techniques such as integration technique, data assimilation and recently using Data Interpolation Empirical Orthogonal Func-

*Corresponding author, E-mail: mfadzil@umt.edu.my

tion (DINEOF) technique.

The DINEOF technique decomposes the spatial-temporal variability into a set of orthogonal functions (Liu and Wang, 2013; Waite and Mueter, 2013; Moradi and Kabiri, 2015). The DINEOF is widely used to reconstruct the variables in seas and oceans based on the pattern from surrounding neighbour stations and also the trend throughout the time series. Furthermore, this technique still works with the missing gap up to 98%, with a slight effect on its precision. However, its accuracy and precision can be increased based on the temporal data set. Therefore, this study chose this technique because of its capability to run with only 2% available data, and improved the technique with longer time series dataset.

In this study, the DINEOF technique is applied to the weekly MODIS-Aqua SST data set to analyse the spatial-temporal distribution of SST and the output was compared with the Advanced Very High Resolution Radiometer (AVHRR) global data. The Moderate Resolution Imaging Spectroradiometer (MODIS) and AVHRR data sets provide high resolution and long term data set which is significant for the El Niño Southern Oscillation (ENSO) events study.

The ENSO contributes a significant impact on SST and marine ecosystem generally. It is a periodic fluctuation in SST and air pressure in every 2–7 years across the Pacific region. It largely affects the weather and dynamic in this region. As the southern SCS also receives influence from the ENSO event, thus it is important to identify the influence of ENSO towards upwelling and thermal front for the fishery industry in this region.

The coastal upwelling largely influences by the alongshore wind stress in order to force the water movement in the area. In the SCS, most of the upwelling events (Vietnam coast, Hainan coast and Peninsular Malaysia coast) occur during the southwest monsoon by taking advantage from southwesterly wind during this period. Previous study by Hong et al. (2009) explained in interannual scale, the coastal upwelling gets weaken or strengthen depends on wind patterns which impacted by the ENSO event. As the upwelling mechanism is significantly influenced by the wind setting. Thus, the condition also manipulated the surface current and affected the SST changes as an indication for the upwelling event.

The upwelling in the ECPM is a wind-driven upwelling which generated by Ekman transport or Ekman pumping mechanism. This upwelling is significantly depending on Ekman pumping with 4.55 $m^3/(s{\cdot}m)$ from total transport of 7.49 $m^3/(s{\cdot}m)$ during the peak upwelling season in August (Kok et al., 2017). This upwelling occurs in the presence of strong southwesterly wind thus with positive wind stress curl, causes the divergence on sea surface, and generates the upward water movement in water column, which is called upwelling event.

Meanwhile, Jing et al. (2011) reported that upwelling in Taiwan Strait became stronger during the El Niño years due to the strong southwesterly wind prevailed along the coast thus it enhanced the forcing in the local upwelling setting and strengthened the upwelling event in the area. The study also compared the upwelling strengths during the El Niño year (1997) in the northern SCS (Hainan coast and Taiwan Strait) and western SCS (Vietnam coast). The finding reveals that during El Niño year the upwelling in the northern SCS was strengthened meanwhile in the western SCS the upwelling was weakened and almost no upwelling occurred during that particular year. This condition is developed by the weak southwest monsoon wind in the western SCS region and strong southerly wind in the northern SCS region due to atmospheric circulation over the SCS and western Pacific region during ENSO event. This defined that the upwelling event is an air-sea interaction mechanism.

This study aims to observe the dynamic of the coastal upwelling event in the ECPM which occurs during the southwest monsoon season and the ENSO effects towards coastal upwelling by using SST from satellite data. This study utilised the MODIS data set from 2005 until 2015 in the southern SCS area hence the DINEOF technique is necessary in order to solve the cloud cover issue in satellite imagery data for this study area.

2 Study area

The southern SCS has a depth less than 100 m with an average of 20–30 m along the ECPM and in the Gulf of Thailand (Fig. 1). The study area range from latitude 1°S to 14°N and longitude 97°E to 108°E . The basin is bordered by the ECPM and the Gulf of Thailand, and involve five countries which are Malaysia, Thailand, Cambodia, Vietnam and Natuna Islands (Indonesia). This basin is classified as shallow shelf area while in term of the coastal slope, the ECPM has a steep coast bathymetric changes as compare to bathymetry in the Gulf of Thailand. The centre of this basin has 50 m water depth in average. This basin also has two openings that connect with other oceans, which links with the Pacific Ocean at the east while links to the Indian Ocean at the south.

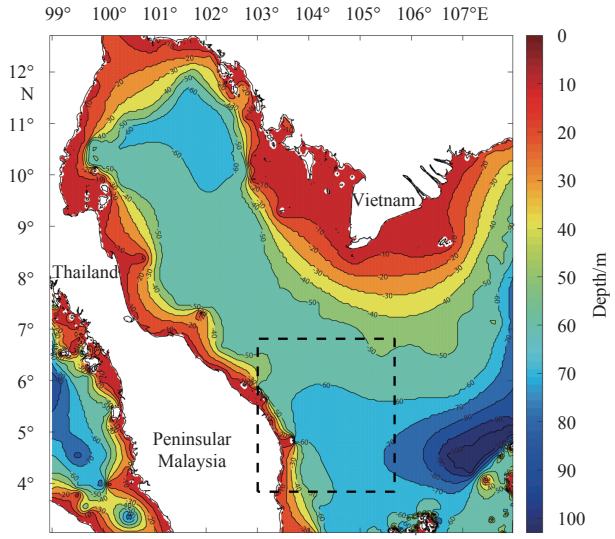

Fig. 1. Bathymetry of the Gulf of Thailand and east coast of Peninsular Malaysia. The dashed box is the upwelling area specified between longitude 103.0°E and 105.6°E, latitude 4°N and 6.4°N.

The study region is categorised as shallow shelf basin as it has less than 60 m water depth along the ECPM coastal waters. Meanwhile, the coastal upwelling and thermal front occur at a specific zone in the southern SCS region. The upwelling area has been defined from the studies done by Akhir et al. (2015) and Kok et al. (2015). This upwelling area (Fig. 1) will be used for detail analysis on upwelling dynamic throughout this study.

3 Data and methods

The SST MODIS-Aqua data set was 4 km resolution Level 3 (L3) mapped weekly from January 2005 to December 2015. The data were downloaded from NASA ocean color website (http://oceandata.sci.gsfc.nasa.gov). The L3 MODIS-Aqua has the bias value of –0.05°C (Montes et al., 2014) and the data were based on

merging daily satellite data for 8 days calculated using a linear interpolation of the daily data and optimum interpolation data. The 11 years of MODIS-Aqua data sets were archived for ECPM area ranged from latitude 8.0°N to 2.5°N and longitude 102°E to 106°E. A total of 495-time series images from January 2005 to December 2015 was then converted into a workable format for processing step.

The general bathymetric chart of the oceans, a global 30 arc-second interval grid data was applied for land and cloud masking on satellite data set. The masking was necessary for data reconstruction technique. The missing data was reconstructed and filled using the DINEOF method (Alvera-Azcárate et al., 2005, 2012, 2016; Liu and Wang, 2013; Moradi and Kabiri, 2015). This method is a reconstruction technique to fill the gap of missing data based on time and frequency transformation. This technique produces a consistent output and is not restricted to a certain parameter. It also consumes less computational time to run using Linux environment.

There were three major steps to run the technique. Firstly, the missing data set into zero and land value set into one. Then, the Empirical Orthogonal Function (EOF) decomposition was calculated by the singular value decomposition (SVD) technique. The missing gaps in the data were filled by reconstruction of the data series using the EOF technique in equation below:

$$X_{i,j} = \sum_{p=1}^{k} S_p (U_p)_i (V_p^{\mathrm{T}})_j,$$

where $X_{i,j}$ is the missing data, i and j are the spatial and temporal of data set, U_p and V_p are the $\boldsymbol{p}$th matrix of the spatial and temporal from EOF, while S_p is the $\boldsymbol{p}$th singular value from SVD, and k is the number of EOF be used in the reconstruction process.

Secondly, the SVD decomposition was computed based on the new prediction matrix data until it obtained the minimum root mean square error (RMSE) between the prediction data and reconstructed data. Throughout this process, the number of EOF (k) was increased.

Thirdly, when the optimal number of EOF was determined, the technique proceeded with cross validation for the entire data set with the initial data. Afterward, final reconstructed values of missing data were determined. This is the general description of the DINEOF technique and for more detail description, see Beckers and Rixen (2003) and Alvera-Azcárate et al., (2005). This study used the SST AVHRR data set from National Oceanic and Atmospheric Administration (NOAA) earth system research laboratory to analyse the 20 years of ENSO event from 1996 to 2015. The SST AVHRR data is an assimilation data set done by NOAA which is a part of the international comprehensive ocean –atmosphere data set where the data was sourced from AVHRR sensor satellite data and field measurement data from ships and floating devices. The data were later produced using linear interpolation of the weekly and optimum interpolation data set. The data set has bias –0.03°C (Reynolds et al., 2002; Khalil et al., 2016).

Afterward, the wavelet transformation (WT) analysis was used to examine the spatial-temporal stability and abnormality of SST in the study area. This method consists of a signal in a hierarchical structure of approximations and detail at each decomposition level. The wavelet of approximation (low-pass) and detail (high-pass) coefficient vectors were generated based on the original signal for each level in this study used up to level seven. The approximation coefficients represented the signal with high scale and low frequency components while detailed coefficients represented the signal of low scale and high frequency components. The whole process generated by a signal as original data, a low-pass as approximation coefficient, a high-pass as detailed coefficient and half-band filter which were used to yield the two sequences. These sequences were then sub-sampled (decimated) by the factor of two due to distinct principle. The process can be repeated as many times as needed on the lower level and it depends on time scale data set. This study used weekly data set for 19 years of time scale therefore it needed seven times repetition to the lower level. This study used the Daubechies wavelet as mother wavelet because it showed acceptable results for oceanography data analysis and has been used in previous studies (Liu et al., 2007; Wang et al., 2009; Moradi and Kabiri, 2015).

4 Results and discussion

4.1 *DINEOF validation*

The output from the DINEOF has to be validated in term of its accuracy and certified the technique in this study. Therefore, this study chose to validate the DINEOF output with another remote sensing data, AVHRR. The AVHRR is a NOAA product of scanning radiometer that widely used for determining cloud cover and the surface temperature including land and sea surface. It has 6 detectors to receive different bands of radiation wavelengths and has up to 1.09 km resolution.

The comparison of the DINEOF was output with the AVHRR data (Fig. 2) which extracted at the same location from both datasets. The result, monthly time series of SST, shows that the DINEOF generally overestimated the SST value, but the variability is highly consistent between the DINEOF output and AVHRR data. The bias value between datasets was 0.17°C which in an acceptable range with 95% significant different. Therefore, the DINEOF output was ratified to be used for further analysis in this study.

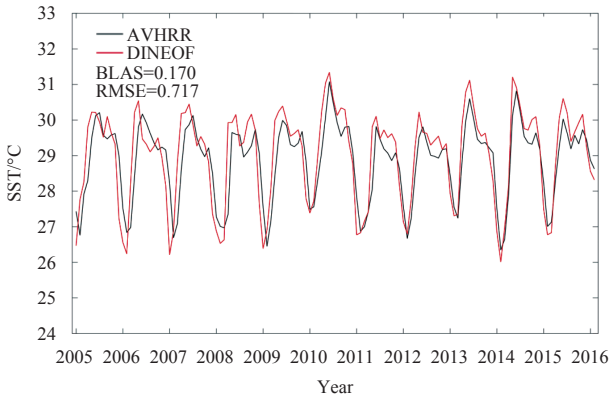

Fig. 2. Validation of DINEOF output with AVHRR dataset.

4.2 *Monthly mean SST distribution*

The annual monthly mean SST distribution is shown in Fig. 3 with the different temperature range of colour bars. This is because of a very high range of temperature differences during the dry season and wet season throughout the years (2005–2015). The maximum temperature reached 33°C and the minimum temperature dropped to 24°C. Therefore, it is difficult to find the constant values to represent colour bar for all the months without wretched the contour plots.

A higher temperature with warm water spotted in May and June while lower temperature and cold water appeared in January and February. Interestingly, in August there was a patch of

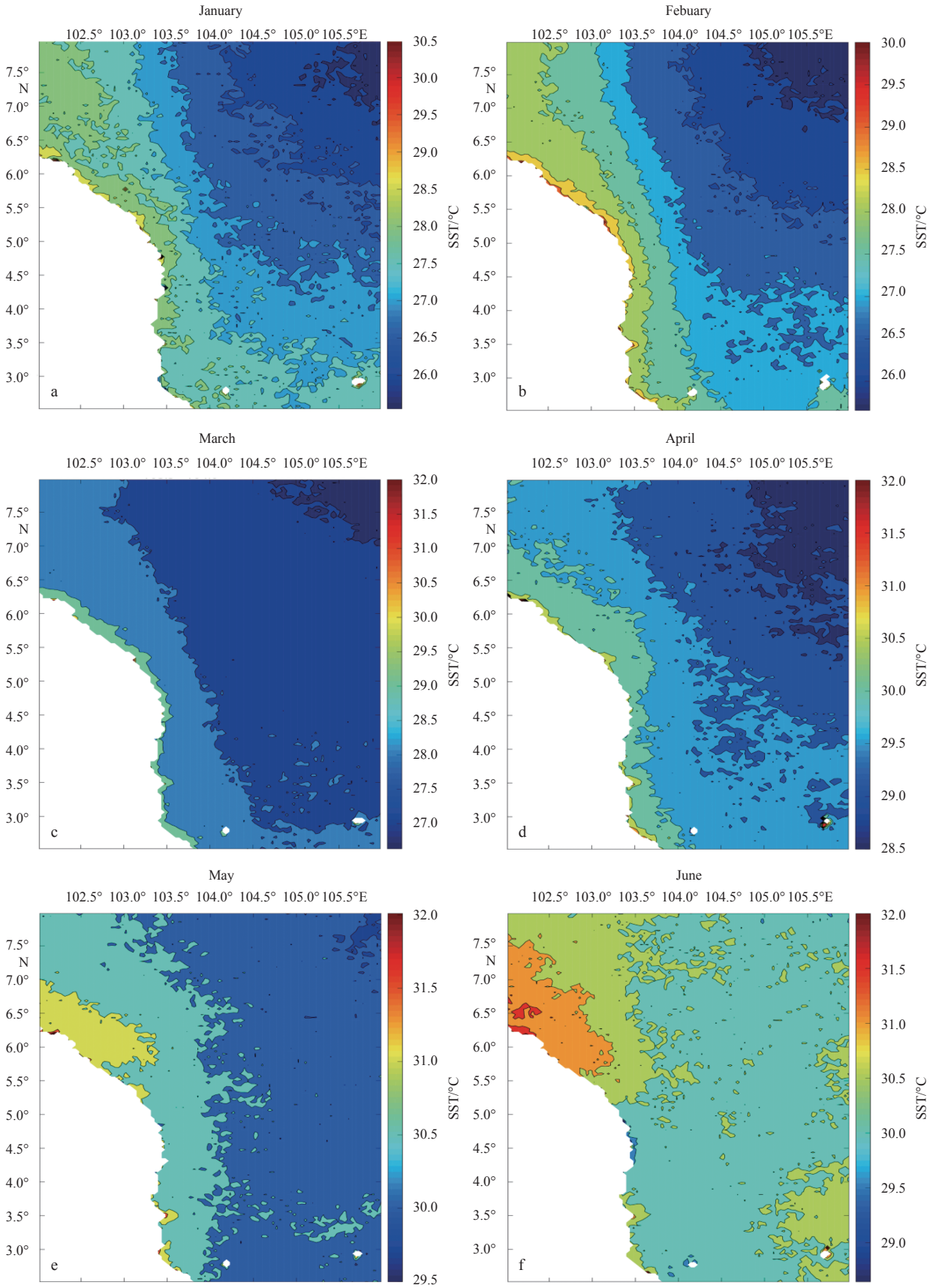
January
Febuary
March
April
May
June
102.5° 103.0° 103.5° 104.0° 104.5° 105.0° 105.5°E
7.5° N
7.0°
6.5°
6.0°
5.5°
5.0°
4.5°
4.0°
3.5°
3.0°
SST/°C
a
b
c
d
e
f

Fig. 3.

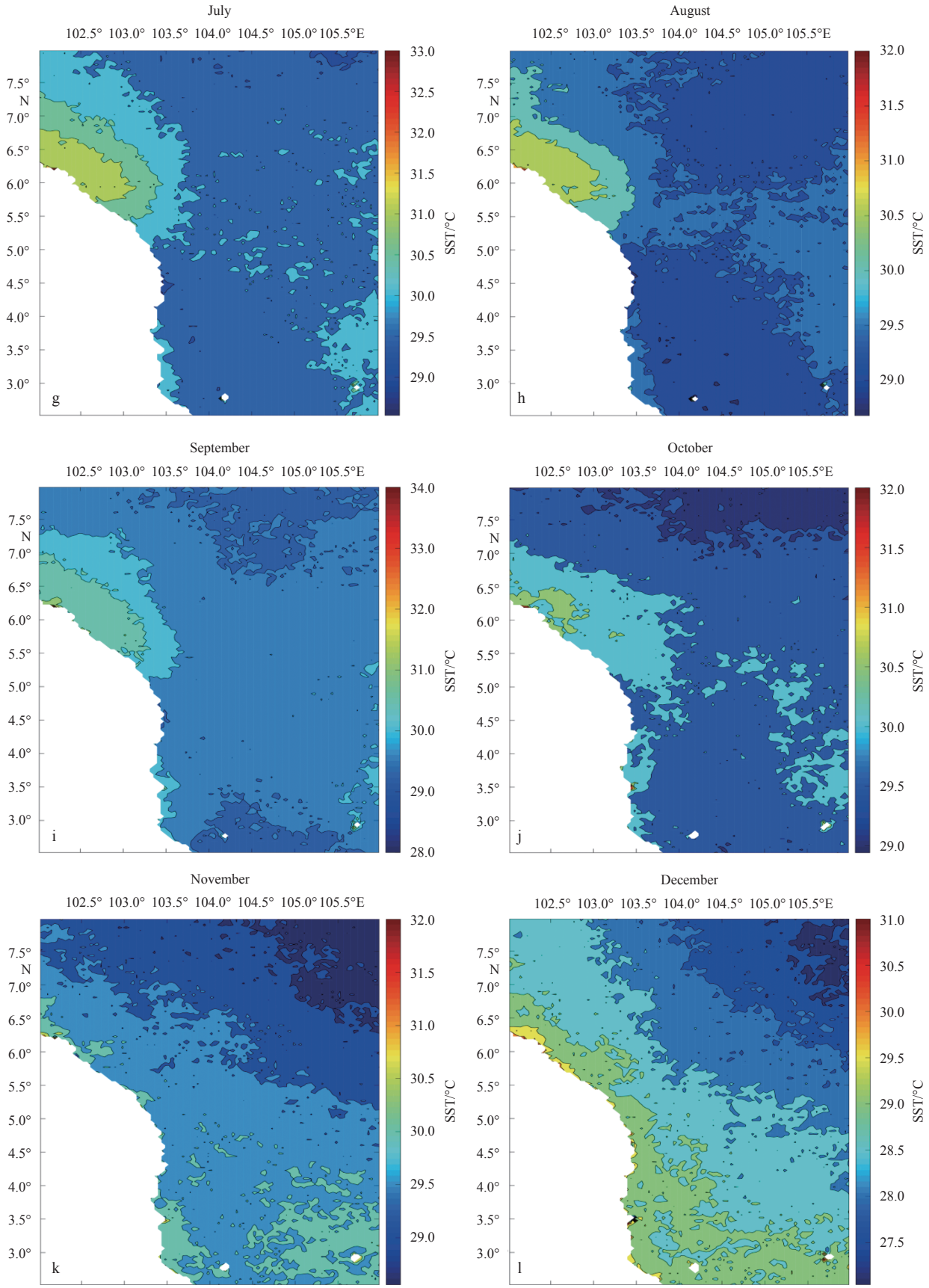

Fig. 3. The annual monthly mean SST (°C) distribution.

cold water at southern ECPM along the southern coast, and also a patch of warm water at northern ECPM along the northern coast, then both of these water patches converged and moved to the north-eastward. This pattern of SST distribution was reported as thermal front and also an upwelling event in the ECPM (Kok et al., 2015; Akhir et al., 2015). Meanwhile, the rest of the months showed the transition of the phases of warm water and cold water according to monsoon seasons.

The distribution of SST clearly shows the temperature changes accordingly to the monsoon seasons. The southwest monsoon occurs from June to September and the west coast of Peninsular Malaysia is largely affected by this monsoon compared to the ECPM. Commonly, there is hot and dry weather before the monsoon coming which normally occurs in May and June. While the northeast monsoon arrives in December to February brings along the cold water from the northern SCS into the southern SCS. During this monsoon season, the ECPM received large influence by this season compared to the west coast of Peninsular Malaysia. March and April were the transition months from the northeast monsoon to the southwest monsoon while October and November were a transition period for the southwest monsoon to the northeast monsoon.

The upwelling event spotted based on a few degrees temperature difference from the surrounding area. In the study region, the SST difference was 2°C between the southern and northern part of ECPM. Figure 4 shows the yearly SST distribution during the peak season of upwelling from 2005 to 2015. In all years except 2009 and 2013, there was a cold-water patch along the ECPM coast ranged from latitude 3°N to 5°N. However, the cold-water patches were different in size throughout the years depending to upwelling strength during the period. This cold water patch was confirmed by Akhir et al. (2015) due to the coastal upwelling process during the southwest monsoon season. Previous studies (Phuoc et al., 2002; Akhir et al., 2015) reported during the southwest monsoon season, a small-scale coastal upwelling event occurred in the ECPM.

This coastal upwelling mechanism is driven by the strong south-westerly wind blows parallel to the coastline and with the Ekman transport moves to the right, thus it provides a good setting for an upwelling event. However, the dynamic of upwelling from the year 2005 to 2015 showed a significant difference in certain years specifically in 2008 and 2013. Figure 5 shows that in 2008 and 2013 the upwelling unclearly spotted with less than a degree (~0.5°C) SST difference. This SST patterns suggest due to the multi-scale of ENSO series in 2007–2008, 2009–2010 and 2012–2013.

4.3 *The ENSO influence in the southern SCS*

Generally, the ENSO has been monitored in the Pacific Ocean and divided into several regions (Niño 4, Niño 3.4 and Niño 3) for SST distribution assessment. Part of that, researchers consider the SST anomaly at Niño 3.4 region for ENSO phenomena reference as it is the middle region. The SST fluctuation due to the ENSO events might be varied between the Pacific Ocean and other small regions such as the Luzon Strait, Taiwan Strait and Sunda Shelf because of the ENSO modulation itself (Chao et al., 1997). In many cases, the effect may be delayed as the ocean take time for heat content and water exchange process. This can explain the SST patterns for the years of 2008, 2009 and 2012 (Fig. 5).

During 2006–2007, there was a moderate of El Niño (refer oceanic Niño index in Fig. 6) thus explained the high SST in 2008 as the study region was far from Niño 3.4 region in Sunda Shelf and ECPM specifically. While in 2009–2010 the ENSO event was defined as unique because it had fast transition phase of warm and cool followed by La Niña in 2011. Due to this unique transition, it also explained the slightly lower SST in study region in 2010 compared to the oceanic Niño index scale and SST in other regions (Kim et al., 2011). With the same reason, it also explained the high SST in 2012 as the La Niña 2011 is followed by the weak El Niño in 2012 (refer oceanic Niño index in Fig. 6). This suggests as the tail-enders from the series of fast transition from the warm to the cool and warm pool of ENSO events in the Pacific Ocean.

In order to observe the temperature difference in upwelling area, this study calculated the mean value specifically in upwelling area (Fig. 5). The area was defined according to previous studies (Akhir et al., 2015; Kok et al., 2015). It suggested that due to strong ENSO event in 2009–2010, the occurrence of the coastal upwelling in ECPM was not clearly seen (Fig. 4) and it is caused by the stratification and atmospheric circulation promoted by the strong El Niño event during the period (Jing et al., 2011). This El Niño promotes high SST thus it creates strong stratification for water column and prevents upwelling event (Riegl et al., 2015). Figure 5 shows the mean SST in upwelling area and the highest SST recorded was in 2010 indicating strong El Niño in 2009–2010. In order to indicate the strength of ENSO, this study observed the oceanic Niño index using 3 months mean SST anomalies based on NOAA data done by Dahlman (2009). Figure 6 presents the oceanic Niño index from 2005 until 2015 with the highest oceanic Niño index in 2015–2016, and indicates strongest El Niño followed by the El Niño in 2009–2010 with nearly strong El Niño and after that fast changed to moderate La Niña.

4.4 *Wavelet analysis*

Previous study by Kim et al. (2011) indicates the 2009–2010 El Niño was unique characteristic due to the fast phase transition to La Niña. Each series of ENSO has different characteristic and scale, thus it gives different impact towards SST and its influence on upwelling event. To understand this in detail, a WT analysis was done using AVHRR NOAA optimum interpolation SST extended time from 1996 until 2015 (Fig. 7). The reason for extending time length was due to considering the influence of a strong El Niño in 1997–1998. This study attempted to compile the series of ENSO for the wavelet analysis in order to compare the signature of El Niño events in 1997–1998, 2009–2010 and 2015–2016.

The WT analysis showed that the approximation levels related to low frequency components while the abnormal or noise signal was presented in detail series which related to high frequency components. The levels of approximation A4, A6 and detail level of D3, D4 and D6 provides information about the seasonal, annual average, weekly, monthly and inter annual abnormality over the year of 1996–2015, respectively (Fig. 7).

In detail level of D7 shows inter-annual abnormality of 26 years (1996–2015) with high peaks in 1997–1998 and 2009–2010 (Fig. 7). This indicates the strong El Niño years in Pacific region specifically region Niño 3.4 based on oceanic Niño index in Fig. 7. While in approximation level of A7, a rose occurred in 1997–1998 and 2015–2016 compared to whole time series. This indicates that El Niño in 1997–1998 is the strongest from the time period, and that of in 2015–2016 is expected to be stronger.

4.5 *Coastal upwelling and thermal front*

The previous study was done by Kok et al. (2015) which reported the presence of the thermal front zone in the ECPM waters during the southwest monsoon season which related with upwelling event. The study suggests that the upwelling event enhanced and strengthen the thermal front in the area. As dis-

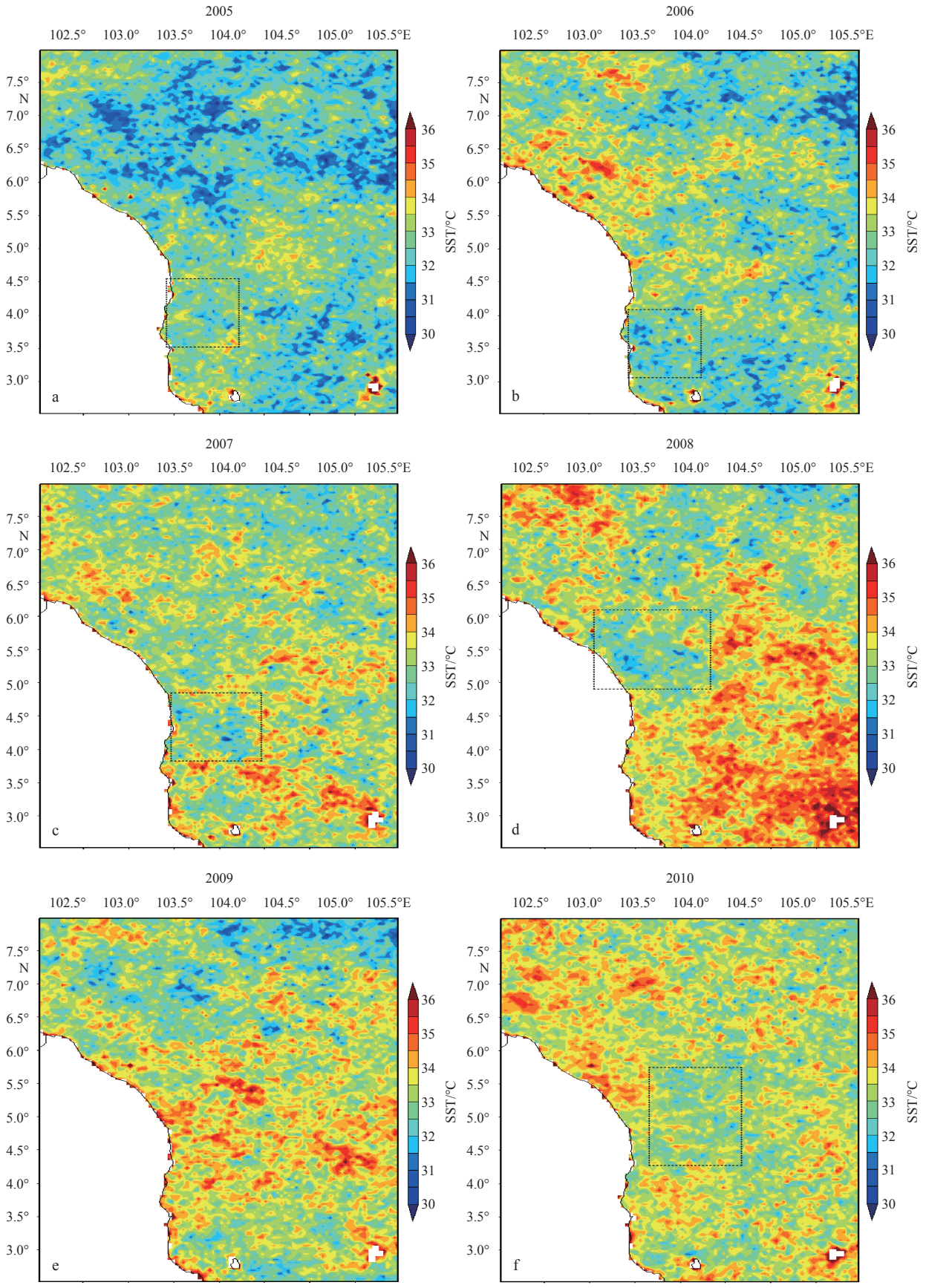
2005
2006
2007
2008
2009
2010
102.5° 103.0° 103.5° 104.0° 104.5° 105.0° 105.5°E
7.5° N 7.0° 6.5° 6.0° 5.5° 5.0° 4.5° 4.0° 3.5° 3.0°
36 35 34 33 32 31 30
SST/°C
a
b
c
d
e
f

Fig. 4.

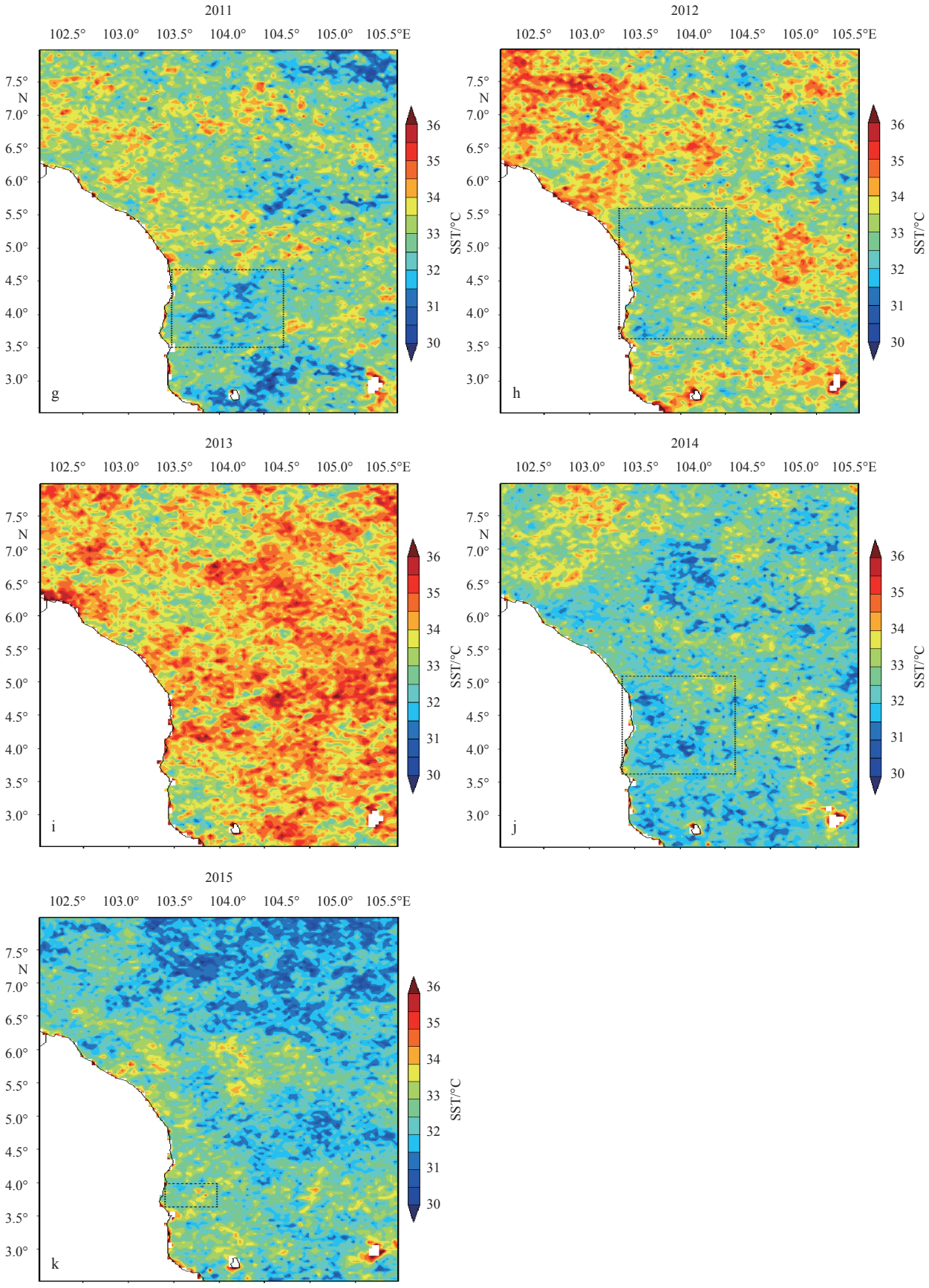

Fig. 4. SST distribution during the peak season of upwelling from 2005 to 2015.

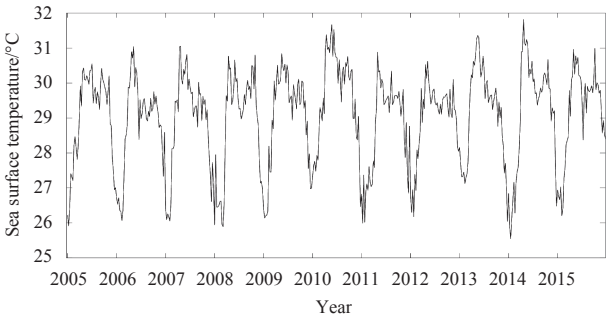

Fig. 5. Mean sea surface temperature in upwelling area from 2005 to 2015.

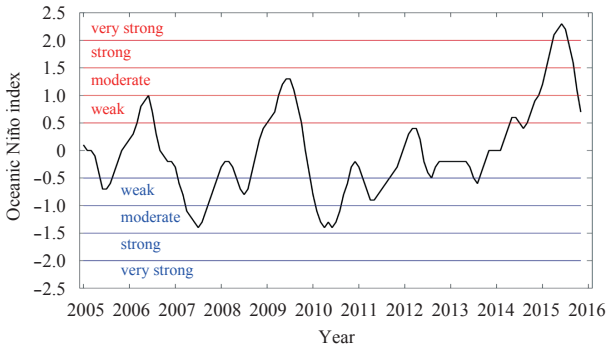

Fig. 6. Oceanic Niño index for 2005 until 2015.

cussed above, the upwelling is significantly affected by El Niño event, thus this study is also interested to investigate the influence of El Niño towards the thermal frontal zone in the ECPM. A SST cross section at the 5.5°N latitude versus longitude from shoreline to 105°E can identify the thermal frontal area border based on sudden temperature changes. The reason of this selection 5.5°N was because the thermal frontal zone ranged between 5°N to 6°N (Fig. 8).

In general, Fig. 9 shows the temperature dropped at 103.8°E, thus it determined the thermal frontal zone border was at this specific longitude. It is clearly seen in August, which discussed before as the strong period for upwelling event, the upwelling event and thermal frontal zone are correlated. This could be an additional evidence to support Kok et al. (2015) argument where upwelling event strengthens the thermal frontal zone occurrence in the ECPM.

The sequence began in June, July and reached its peak in August which was during the southwest monsoon season. However, the temperature dropped weakly and almost no changes in December, January and February, which had the northeast mon-

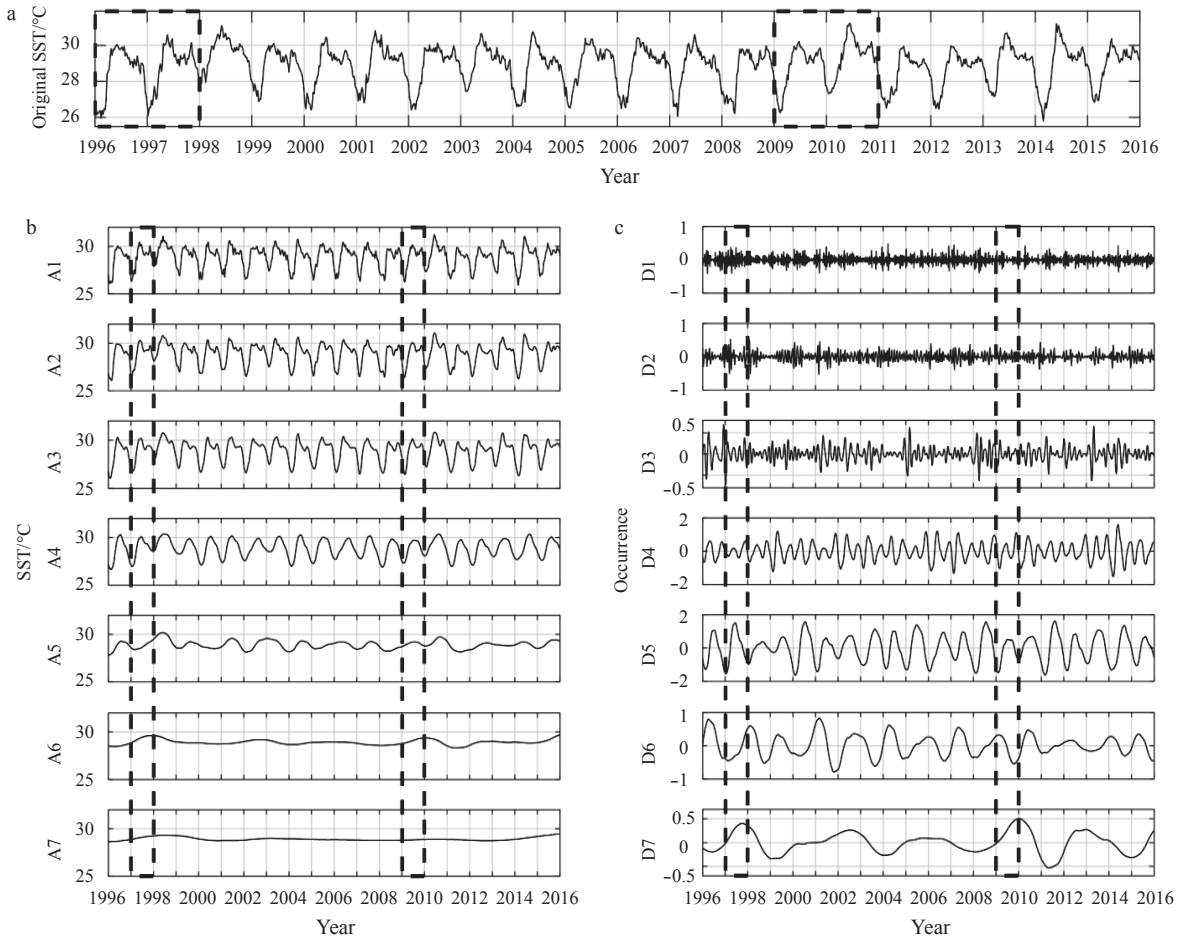

Fig. 7. Wavelet transformation analysis for the SST in study region. a. Original monthly mean SST in study region, b. the approximation series related to the frequency components, and c. the detail series related to fluctuation components. A represents the approximation level, while D shows the detail lavel.

soon influence during this period. This suggests the strong northeast monsoon wind created well mix in the water column for the SCS basin and the ECPM waters specifically. The separation of warm and cool water occurred at the 103°E–104°E along the ECPM.

5 Conclusions

The coastal upwelling and thermal front zone at the southern SCS and the ECPM specifically are connected and generated by a single mechanism. The coastal upwelling driven by the strong southwest monsoon wind and the cold water caught the northward monsoon current to Vietnam. Meanwhile, the warm water

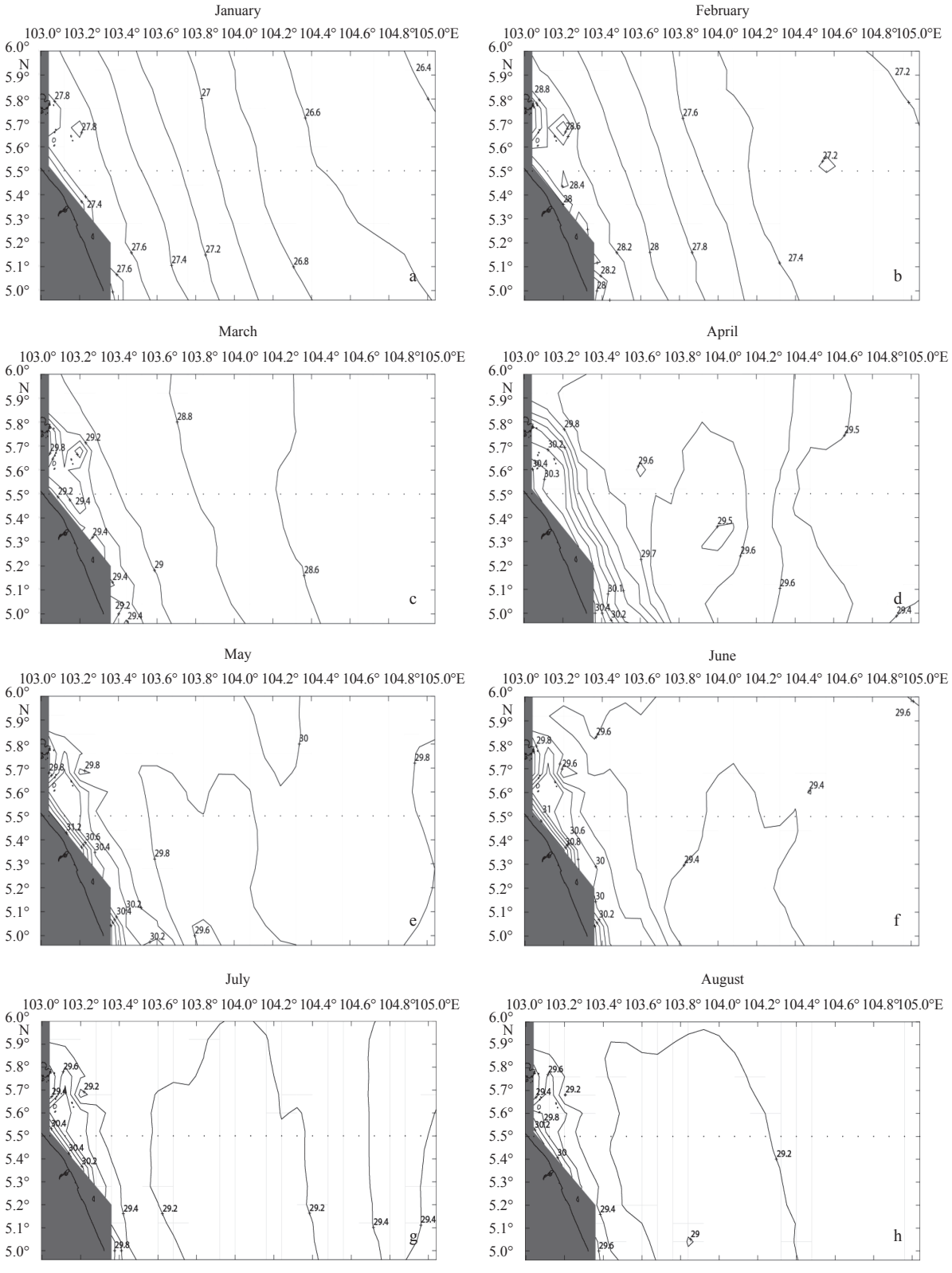

Fig. 8.

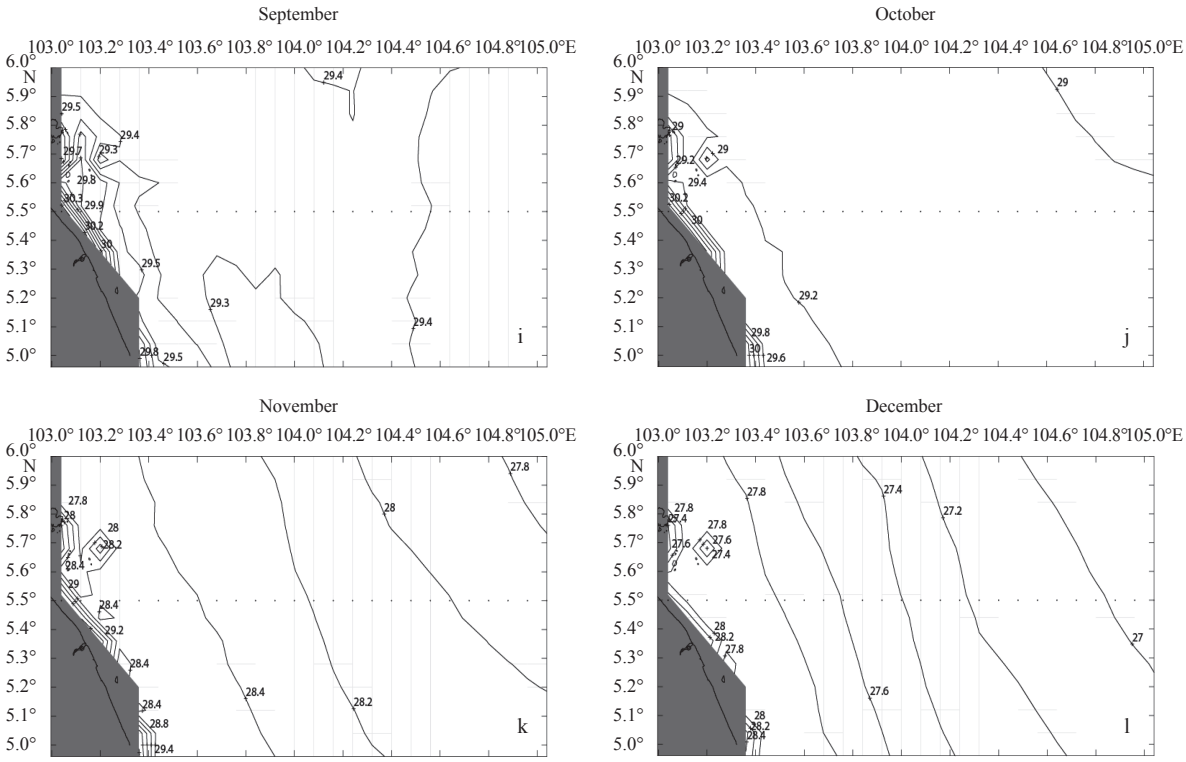

Fig. 8. Yearly month mean SST (°C) distribution from 1996 to 2015 (January–December).

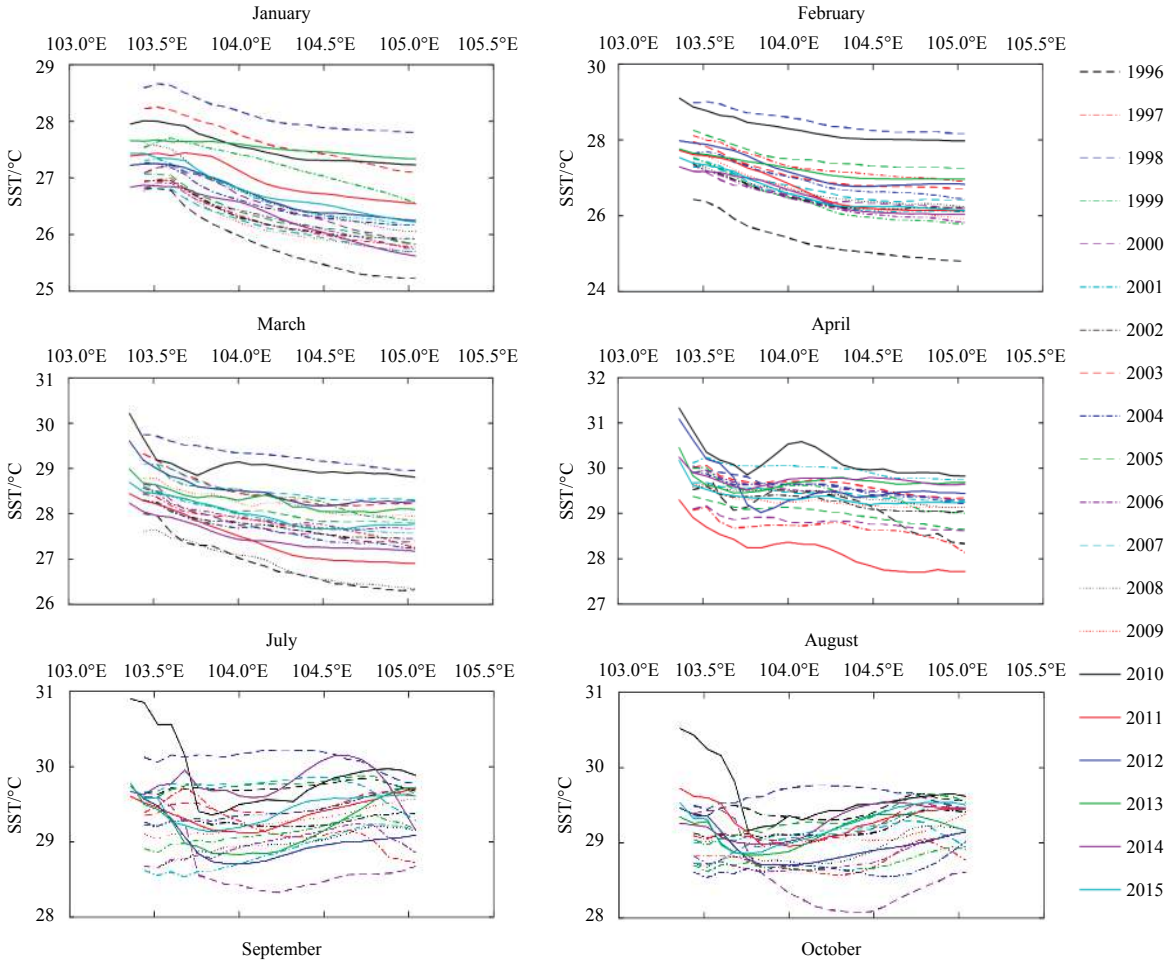

Fig. 9.

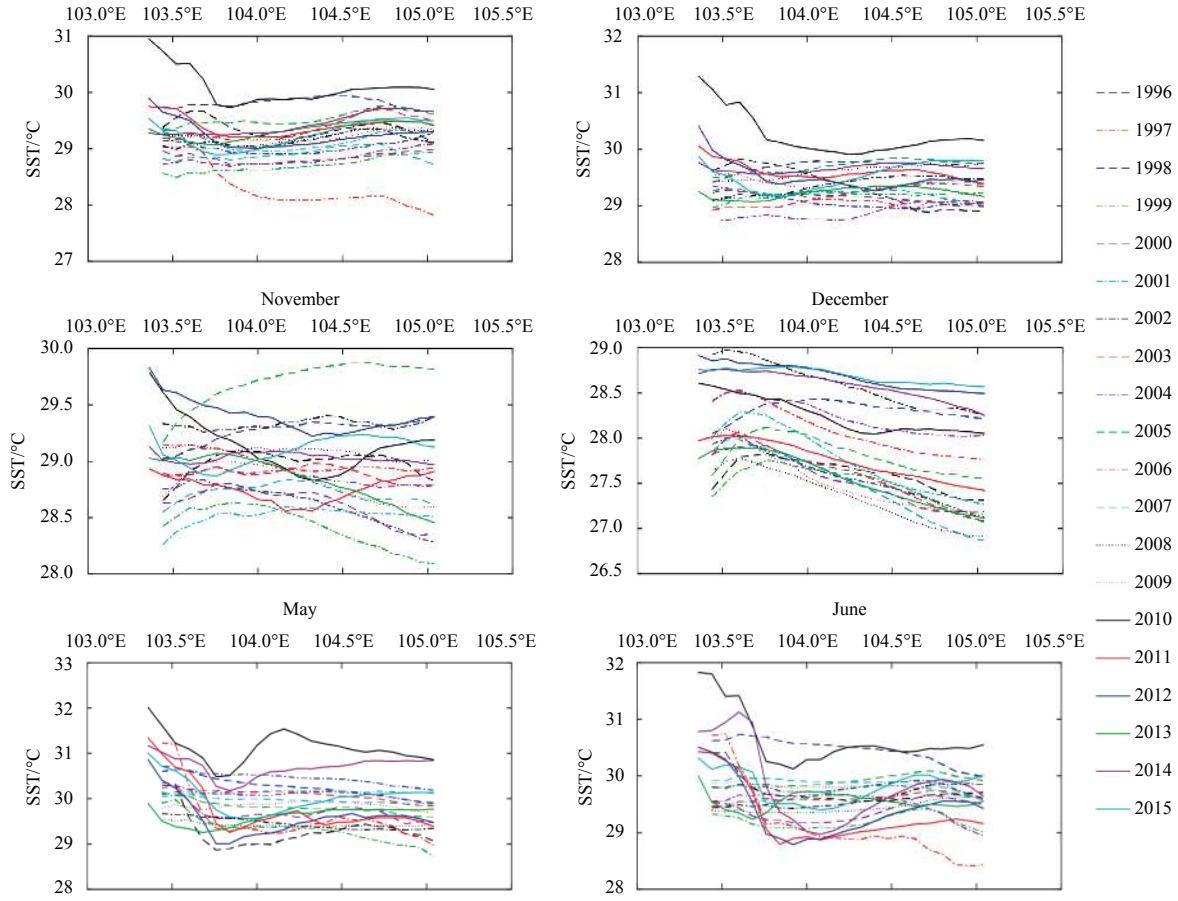

Fig. 9. Monthly mean SST with cross section at 5.5°N latitude from shoreline to 105°E (January–December).

from the Gulf of Thailand flowed parallel with cold water from the ECPM in the same northward monsoon current. Therefore, it was creating the thermal front zone in the ECPM. However, this mechanism is fully depending on strong monsoon wind and this type of coastal upwelling in shallow shelf area may easily be disturbed by high temperature range from ENSO events.

The SST MODIS–Aqua data from 2005–2015 were archived and reconstructed using the DINEOF technique and analysed using the WT analysis. The WT analysis shows the spatial-temporal SST stability and abnormality throughout the time period. The variability of the distribution of SST significantly influences by the ENSO events thus it also affects the upwelling dynamics in the ECPM.

As a conclusion, the DINEOF and WT methods can be considered as the essential tools for assessment of the spatial-temporal distribution of SST in the study region. Moreover, the findings reveals that upwelling region in the ECPM significantly influenced by El Niño event. It is clear that a detail future work is required for better understanding of the upwelling in ECPM in term of water column mixing and the Gulf circulation which affects the upwelling and thermal front zone formation.

Acknowledgements

We acknowledge the Institute of Oceanography and Environment, Universiti Malaysia Terengganu for high specification of computer and good facilities for retrieved data, storage and run the analyses for this study. The MODIS data was obtained from NASA Ocean Color website and AVHRR-OI data was from NOAA website. The DINEOF technique was from the geohydrodynamics and environment research website. This work was supported by the UMT (INOS-HICoE).

References

Akhir M F, Daryabor F, Husain M L, et al. 2015. Evidence of upwelling along peninsular malaysia during southwest monsoon. Open Journal of Marine Science, 5(3): 273–279, doi: 10.4236/ojms.2015.53022

Alvera-Azcárate A, Barth A, Parard G, et al. 2016. Analysis of SMOS sea surface salinity data using DINEOF. Remote Sensing of Environment, 180: 137–145, doi: 10.1016/j.rse.2016.02.044

Alvera-Azcárate A, Barth A, Rixen M, et al. 2005. Reconstruction of incomplete oceanographic data sets using empirical orthogonal functions: Application to the Adriatic Sea surface temperature. Ocean Modelling, 9(4): 325–346, doi: 10.1016/j.ocemod.2004.08.001

Alvera-Azcárate A, Sirjacobs D, Barth A, et al. 2012. Outlier detection in satellite data using spatial coherence. Remote Sensing of Environment, 119: 84–91, doi: 10.1016/j.rse.2011.12.009

Beckers J M, Rixen M. 2003. EOF calculations and data filling from incomplete oceanographic datasets. Journal of Atmospheric and Oceanic Technology, 20(12): 1839–1856, doi: 10.1175/1520-0426(2003)020<1839:ECADFF>2.0.CO;2

Chao S Y, Shaw P T, Wu S Y. 1997. El Niño modulation of the South China Sea circulation. Progress in Oceanography, 38(1): 51–93

Dahlman L. 2009. NOAA Climate Variability: Oceanic Niño Index. https://www.climate.gov/news-features/understanding-climate/climate-variability-oceanic-niño-index [2016-07-21]

He Shuangyan, Huang Daji, Zeng Dingyong. 2016. Double SST fronts observed from MODIS data in the East China Sea off the Zhejiang-Fujian coast, China. Journal of Marine Systems, 154:

93–102, doi: 10.1016/j.jmarsys.2015.02.009

Hong Huasheng, Zhang Caiyun, Shang Shaoling, et al. 2009. Interannual variability of summer coastal upwelling in the Taiwan Strait. Continental Shelf Research, 29(2): 479–484, doi: 10.1016/j.csr.2008.11.007

Jing Zhiyou, Qi Yiquan, Du Yan. 2011. Upwelling in the continental shelf of northern South China Sea associated with 1997–1998 El Niño. Journal of Geophysical Research: Oceans, 116(C2): C02033

Khalil I, Atkinson P M, Challenor P. 2016. Looking back and looking forwards: Historical and future trends in sea surface temperature (SST) in the Indo-Pacific region from 1982 to 2100. International Journal of Applied Earth Observation and Geoinformation, 45: 14–26, doi: 10.1016/j.jag.2015.10.005

Kim W, Yeh S W, Kim J H, et al. 2011. The unique 2009–2010 El Niño event: A fast phase transition of warm pool El Niño to La Niña. Geophysical Research Letters, 38(15): L15809

Kok P H, Akhir M F M, Tangang F, et al. 2017. Spatiotemporal trends in the southwest monsoon wind-driven upwelling in the southwestern part of the South China Sea. PLoS One, 12(2): e0171979, doi: 10.1371/journal.pone.0171979

Kok P H, Akhir M F M, Tangang F T. 2015. Thermal frontal zone along the east coast of Peninsular Malaysia. Continental Shelf Research, 110: 1–15, doi: 10.1016/j.csr.2015.09.010

Liu Yingchun, Santos A, Wang S M, et al. 2007. Tsunami hazards along Chinese coast from potential earthquakes in South China Sea. Physics of the Earth and Planetary Interiors, 163(1–4): 233–244

Liu Dongyan, Wang Yueqi. 2013. Trends of satellite derived chlorophyll-a (1997–2011) in the Bohai and Yellow Seas, China: Effects of bathymetry on seasonal and inter-annual patterns. Progress in Oceanography, 116: 154–166, doi: 10.1016/j.pocean.2013.07.003

Montes I, Dewitte B, Gutknecht E. 2014. High - resolution modeling of the Eastern Tropical Pacific oxygen minimum zone: Sensitivity to the tropical oceanic circulation. Journal of Geophysical Research: Oceans, 119(8): 5515–5532, doi: 10.1002/2014JC009858

Moradi M, Kabiri K. 2015. Spatio-temporal variability of SST and Chlorophyll-a from MODIS data in the Persian Gulf. Marine Pollution Bulletin, 98(1–2): 14–25

Phuoc T, van Lanh V, Long B H, et al. 2002. Main Structures of Sea Surface Temperature (SST) in South China Sea from Satellite Data. In: Asian Conference on Remote Sensing (ACRS). Hanoi: Asian Association on Remote Sensing

Reynolds R W, Rayner N A, Smith T M, et al. 2002. An improved in situ and satellite SST analysis for climate. Journal of Climate, 15(13): 1609–1625, doi: 10.1175/1520-0442(2002)015<1609:AIISAS>2.0.CO;2

Riegl B, Glynn P W, Wieters E, et al. 2015. Water column productivity and temperature predict coral reef regeneration across the Indo-Pacific. Scientific Reports, 5: 8273, doi: 10.1038/srep08273

Waite J N, Mueter F J. 2013. Spatial and temporal variability of chlorophyll-a concentrations in the coastal Gulf of Alaska, 1998–2011, using cloud-free reconstructions of SeaWiFS and MODIS-Aqua data. Progress in Oceanography, 116: 179–192, doi: 10.1016/j.pocean.2013.07.006

Wang Bin, Huang Fei, Wu Zhiwei, et al. 2009. Multi-scale climate variability of the South China Sea monsoon: A review. Dynamics of Atmospheres and Oceans, 47(1–3): 15–37